Chemical Engineering Journal 248 (2014) 422–429

Contents lists available at ScienceDirect

Chemical Engineering Journal

journal homepage: www.elsevier.com/locate/cej

The oxidation of heavy oil to enhance oil recovery: The numerical model and the criteria to describe the low and high temperature oxidation

Yue Chu [a], Cheng Fan [a], Qiang Zhang [a,*], Cheng Zan [b], Desheng Ma [b], Hang Jiang [b], Yao Wang [a], Fei Wei [a]

[a] Beijing Key Laboratory of Green Chemical Reaction Engineering and Technology, Department of Chemical Engineering, Tsinghua University, Beijing 100084, China
[b] State Key Laboratory of Enhanced Oil Recovery, Research Institute of Petroleum Exploration & Development, China National Petroleum Corporation, Beijing 100007, China

HIGHLIGHTS

- A model to describe the temperature distribution of heavy oil oxidation.
- The high- and low-temperature oxidation processes.
- KP and HP factors are proposed to describe the oxidation reaction strength.

GRAPHICAL ABSTRACT

A mathematical model to describe the temperature distribution during the oxidation of heavy oil. Both KP and HP factors are proposed as the criteria to determine the strength of the oxidation reactions.

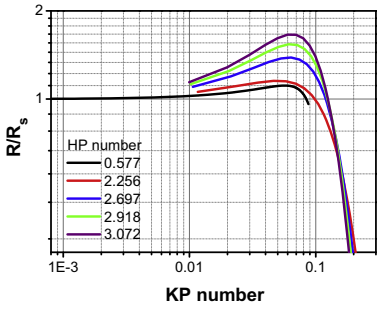

ARTICLE INFO

Article history:
Received 16 January 2013
Received in revised form 7 March 2014
Accepted 11 March 2014
Available online 26 March 2014

Keywords:
Heavy oil
Recovery
Numerical simulation
High temperature oxidation
Low temperature oxidation
Governing dimensionless number

ABSTRACT

The *in situ* oxidation of heavy oil brings exothermic reaction between the hydrocarbon and the oxygen, which renders advantages in high efficiency in heat utilization and displacement for oil recovery. The simulation of oxidation is very convenient to investigate the influence of operation parameters and reflect the dynamic response. In this contribution, a mathematical model to simulate the temperature distribution during the oxidation of heavy oil with the injection wells and the production wells arranged in the hexagonal pattern was developed. The effects of convection, diffusion, oxidation reaction, and coking were considered. The temperature distributions in the high- and low-temperature oxidation processes were simulated. The results exhibited that the modeling domain can be heated by both processes. The significant change in the kinetic parameters of oxidation and coking with temperature induced the different oxidation behaviors between the high- and low-temperature oxidation processes. Two dimensionless parameters, KP and HP factor, were proposed based on the simulation results as the criteria to determine the strength of the oxidation reactions in the enhanced oil recovery process.

1. Introduction

Heavy oil which possesses high content of asphaltene and high viscosity is an important feedstock the resources of which are nearly three times those of the conventional oil [1,2]. Nowadays, more and more attention has been paid on the recovery of heavy oil as the conventional reserves decline significantly. The cost-effective production and processing of heavy oil remains to be a much sought after prize [3].

The recovery of the heavy oil is a complex process because of the high viscosity, high density, and low fluidity properties [4–6].

* Corresponding author. Tel.: +86 10 6278 9041; fax: +86 10 6277 2051.
E-mail address: zhang-qiang@mails.tsinghua.edu.cn (Q. Zhang).

http://dx.doi.org/10.1016/j.cej.2014.03.036
1385-8947/

Nomenclature

A	pre-exponential factor in the oxidation reaction, s^{-1}
A_c	pre exponential factor in the coking reaction, h^{-1}
c	oxygen concentration, mol m^{-3}
c_g	heat capacity of gas, J kg^{-1} K^{-1}
c_s	heat capacity of solid, J kg^{-1} K^{-1}
c_{coke}	weight percentage of produced coke, 1
c_{oil}	weight percentage of heavy oil, 1
c_s	oxygen concentration in the injection well, mol m^{-3}
D	effective diffusion coefficient, m^2 s^{-1}
d_e	diameter of rock particles, m
E	activation energy in the oxidation reaction, J mol^{-1}
E_c	activation energy in the coking reaction, J mol^{-1}
F	mass generated by the oxidation reaction, kg m^{-3} s^{-1}
k	oxidation reaction rate constant, s^{-1}
L	distance from the injection well, m
M_c	molar weight of carbon, kg mol^{-1}
m	mass of the heavy oil in the TG, kg
N	molar flux of oxygen in the TG, mol s^{-1}
P_0	initial pressure in the reservoir, Pa
P_{IW}	pressure of the injection well, Pa
P_{EW}	pressure of the production well, Pa
P_{TG}	pressure in the TG reactor, Pa
Q	heat generated by the oxidation reaction, J m^{-3} s^{-1}
R	rate of oxidation reaction, mol m^{-3} s^{-1}
T_0	initial temperature in the reservoir, K
T_{TG}	temperature in the TG reactor, K
T_s	ignition temperature, K
u	gas velocity, m s^{-1}

Greek letters

β	HP dimensionless number, dimensionless
ε	porosity of the reservoir, dimensionless
η	viscosity of the gas phase, Pa s
κ	gas permeability, m^2
λ	thermal conductivity, W m^{-1} K^{-1}
ρ_s	density of the rocks, kg m^{-3}
ρ_g	density of the gas, kg m^{-3}
φ	KP dimensionless number, dimensionless
ΔP	pressure drop between the injection and producing wells, Pa
ΔH	molar reaction heat, J mol^{-1}

The thermal enhanced oil recovery is proposed based on the characterization of the heavy oil that the oil viscosity can be reduced by several orders of magnitude through the increase of temperature [7]. Based on the mechanism of energy generated, the thermal enhanced oil recovery (EOR) falls into two types: for the former, like steam huff and puff process, the thermal energy at ground is transported into the reservoir to improve its fluidity; in the latter process, oxidative gas is injected into the reservoir and the heat is *in situ* generated by the exothermic reactions between the hydrocarbon and the oxygen (such as the *in situ* combustion) [8–11]. The latter process brings many advantages such as a high efficiency in heat utilization, highly efficient displacement drive mechanism, and less total environmental impact [7].

The oxidation reactions of hydrocarbon were classified as high temperature oxidation (HTO) that occurs at temperatures above 350 °C and low temperature oxidation (LTO) that corresponds to temperatures lower than 350 °C [12]. In the HTO process, the heavy oil is fired, in which the carbon–hydrogen bonds are broken and water and carbon dioxide were produced [13], therefore, continuous combustion is guaranteed, the huge amount of heat release during the underground combustion facilitates the temperature of the reservoir higher than 600 °C. While in the LTO process, it is believed that LTO reactions produce oxygenated hydrocarbons such as carboxylic acids and sulfones with negligible amounts of carbon oxides [14–16]. Although the reaction mechanism is very complex [17], the released reaction heat is beneficial to increase the temperature of reservoir, therefore, the temperature of the whole reservoir is controlled to be lower than the ignition point of heavy oil to thermally reduce the viscosity of the heavy oil to a required level and simultaneously avoid coke generation at high temperature. The LTO process renders advantages on the high efficiency of energy utilization [1,18]. Both the HTO and LTO are very important since their products play a significant role with respect to the sustainability of the combustion process. The use of heterogeneous catalysts is a promising way to mediate the reaction pathway and related characters [13,19]. In most cases, the temperature is a very important index to describe the HTO and LTO with different reaction mechanisms. However, the synergy between the reaction and transport phenomena is not well illustrated yet. If the important parameters in the EOR process are integrated to dimensionless number, the correlation between the strength of the oxidation reaction and the dimensionless number is anticipated to serve as the guidance for choosing rational operation region.

Attributed from the numerous operation parameters and the complex conditions in the heavy oil reservoir, the physical and mathematical simulation becomes necessary before experiments in the field [16,20–24]. The mathematical simulation is widely investigated because of its convenience in studying the influence of operation parameters and reflecting the dynamic response [15,19,22,25–29]. In this work, a mathematical model to describe the EOR process is developed. The conservation of momentum, mass, and energy is considered. The kinetic sub-model is set up based on the characterization of the heavy oil using thermal gravimetric analysis (TGA) with differential scanning calorimeter (DSC). The temperature distribution in the modeling domain is investigated both in HTO and LTO processes. The similarities and differences in the temperature distribution in the two processes are explored. The KP and HP Number are proposed as the dimensionless numbers to describe the oxidation behavior.

2. Mathematical model and numerical simulations

Air was employed as the oxidizing gas to improve oil recovery in the thermal enhanced oil recovery. The injection wells and the production wells are usually located in a meshwork [18,30,31]. Herein wells with hexagonal shaped arrangement are modeled based on the laboratory scale experiment. The six injection wells are located on the points with one producing well in the center as shown in Fig. 1a. The modeling domain is reduced to a 2D geometry (Fig. 1b) only considering the horizontal temperature, concentration, and velocity distribution. The wells are separated from the surrounded rocks by an outside boundary Γ_D. Circle boundary is used to guarantee that the same distances between the injections wells and the outside boundary. The distance between the injection wells (Γ_{IW}) and the production wells (Γ_{EW}) is 1.0 m. The outside boundary (Γ_D) is 0.5 m away from the injection wells.

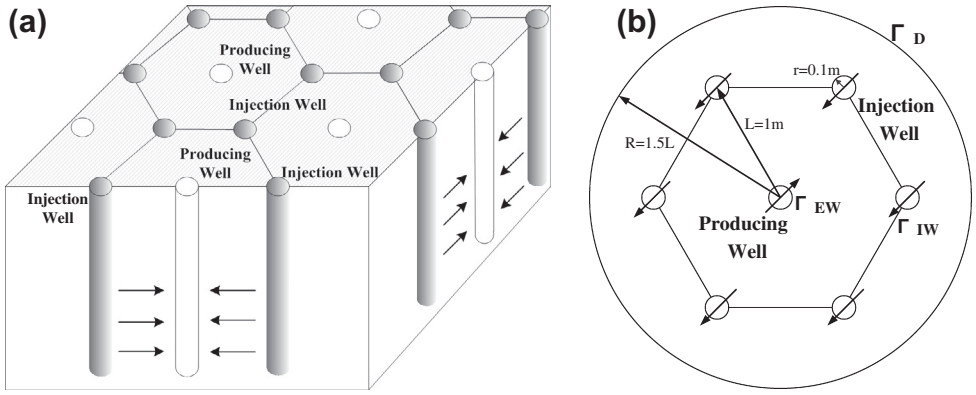

Fig. 1. The arrangement of wells in the oxidation reaction enhanced oil recovery process: (a) 3D illustration of the field; and (b) 2D modeling domain.

The governing equations in the modeling domain contain the conservation equations of momentum, mass and energy. The oxygen mass balance is given by:

$$\partial c/\partial t + \nabla \cdot (-D\nabla c) = R - \mathbf{u} \cdot \nabla c \tag{1}$$

where c is the concentration of oxygen, D is the efficient diffusion coefficient, R is the rate of oxidation reaction, $\mathbf{u}$ is the gas velocity.

The energy balance equation is represented by:

$$(1-\varepsilon)\partial(c_s\rho_s T)/\partial t - \nabla \cdot (-\lambda \nabla T) = Q - \rho_g c_g \mathbf{u} \cdot \nabla T \tag{2}$$

where ε is the porosity of the reservoir, c_s and ρ_s is the heat capacity and density of the rocks, λ is the thermal conductivity, Q is the heat generated by the oxidation reaction, c_g and ρ_g is the gas heat capacity and density.

The conservation equation of momentum is described by:

$$\partial(\rho_g \varepsilon)/\partial t + \nabla \cdot (\rho_g(-\kappa/\eta \nabla p)) = F \tag{3}$$

where κ is the gas permeability, η is the gas viscosity, P is the pressure, F is the mass generated by the oxidation reaction.

To quantitatively describe the reaction and transport phenomena, following assumptions are accepted in this model:

1. The movement of the gas follows the Darcy's law, and the gravity effect is negligible;
2. Ideal gas assumption for the gas phase;
3. The temperature of the reservoir is uniform, indicating that heat transfer between the solid particles and the gas is sufficient fast;
4. The solid phase is stationary during the oxidation process. The Fick's law is used to describe the oxygen diffusion;
5. The oil reservoir is homogeneous distributed in the modeling domain.
6. Water is not considered in the reservoir in this work. Consequently, the heat of vaporization of water is not involved in the energy balance equation.
7. The mode of hot air injection is directly introduced, that is, the temperature of the injection well is constant in the set of boundary conditions.

2.1. Kinetic sub-model of the oxidation reaction

The mass loss and exothermic effect of the heavy oil during the oxidation reaction in the temperature range of 30–500 °C is collected by thermal gravimetric analysis (TGA) with differential scanning calorimeter (DSC) using the Netzsch STA 409 system. The kinetic parameters are determined based on the experimental results. The heavy oil used in the experiment is from Xinjiang Oilfield. The H/C ratio is *ca.* 1.5. The complete combustion of the hydrocarbon with oxygen was carried out in the heavy oil oxidation process [32]. Therefore, the reaction equation is anticipated as follows:

$$CH_{1.5}(s) + 1.375O_2(g) \rightarrow CO_2(g) + 0.75H_2O(g) \tag{4}$$

Assuming that the oxidation reaction is one-order [33], the kinetic equation is given by:

$$dc/dt = kc \tag{5}$$

Assuming Arrhenius behavior, we have:

$$dc/dt = A\exp(-E/RT)c \tag{6}$$

Based on the TGA-DSC characterization result, the rate of oxygen consuming dc/dt can be related to the mass reduction of heavy oil as follows:

$$\frac{dc}{dt} = 1.375\frac{p_{TG}}{M_C N R T_{TG}}\frac{dm}{dt} \tag{7}$$

where P_{TG} is the pressure of the reactor of the thermal gravimetric apparatus, Mc is the molar weight of carbon, N is the molar flux of oxygen in the TGA experiment. The parameter, 1.375, is decided based on the reaction equation.

To obtain the kinetic parameters (A and E) conveniently, taking the logarithm of (1–7) gives:

$$\ln\left(-\frac{1.375}{M_C N}\frac{dm}{dt}\right) = \ln(-A) - \frac{E}{RT} \tag{8}$$

The characterization result of the heavy oil using TGA-DSC with a temperature rising rate of 5 °C min^{-1} is shown in Fig. 2a.

The HTO reactions mainly consist of carbon–hydrogen bond breakage with violent reactions occur and the TG curve exhibits a sharp weight loss and the production of water and carbon dioxide and the LTO reactions lower than 350 °C produce oxygenated hydrocarbons such as carboxylic acids and sulfones with gentle weight loss and a small amount of released reaction heat [13,32]. Although there is no specific trend of the TG curve in the whole temperature range, the distributed activation energy model was efficient to obtain accurate kinetic parameters of oxidation reactions from 30 to 550 °C [34], however, it is very difficult to incorporate the results to the current model. Herein, the kinetic parameters are fitted well at the two temperature intervals respectively as shown in Fig. 2b. The values of $\ln(-1.375/M_C N \cdot dm/dt)$ at different temperatures are available. The kinetic parameters are available by linear fitting (Table 1). The kinetic parameters are fitted separately at two temperature ranges.

The molar reaction heat of the heavy oil oxidation is highly depended on the reaction temperature. The integration of the DSC

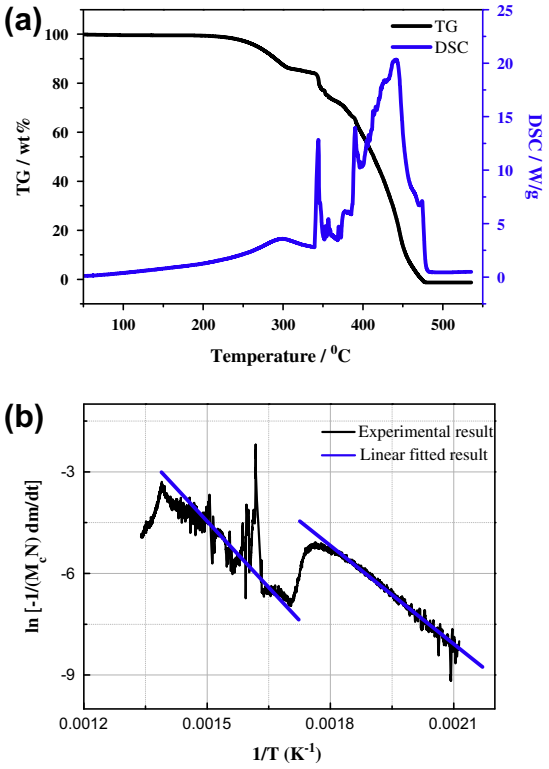

Fig. 2. (a) TGA-DSC characterization results of the heavy oil; (b) linear fitting at two temperature ranges of the TG experimental result after logarithmic treatment. (The flux of gas inlet: O_2: 90 mL min^{-1}, N_2: 10 mL min^{-1}).

Table 1
The fitted kinetic parameters of the heavy oil oxidation reaction.

Temperature range °C^{-1}	200–306	306–500
A (1 s^{-1})	-2.12×10^5	-3.14×10^6
E (J mol^{-1})	8.05×10^4	1.07×10^5

profile provides the molar reaction heat that is fitted using an exponential function as follows [35]:

$$\Delta H(\mathrm{J/mol}) = 6.72 \times \exp\left(\frac{T}{90.93}\right) - 160.93 \tag{9}$$

2.2. Coking sub-model of the heavy oil

There are significant coking formation reactions during the oxidation of heavy oil at high temperatures [18]. The formation of coke blocks the porosity in the reservoir, hindering the flow and diffusion of oxygen. Herein the one-order reaction and Arrhenius assumption which is commonly used in the kinetics of coke generation in the delayed coking process are adopted [36–38]. The thermal cracking of the petroleum residue in the delayed coking process is similar to that the heavy oil undergoes in the HTO process. The kinetic equation of coking reaction is employed as:

$$dc_{coke}/dt = A_C \exp(-E_C/RT) c_{oil} \tag{10}$$

where c_{coke} is the weight percentage of produced coke, c_{oil} is the weight percentage of heavy oil, A_c is the pre-exponential factor of coke formation with a value of 1.4812×10^{24} h^{-1}, while E_c is the correlated activation energy of 348.7 kJ mol^{-1} which are assigned based on the kinetic parameters in the coking reaction of Sudan heavy oil [37].

The formation of coke induces the decrease of reservoir porosity, which further influences the gas permeability. The Ergun equation that is commonly employed to determine the pressure drop of porous medium is applied herein to describe the effect of coking on permeability [39]:

$$K_{Coke} = \frac{\varepsilon_C^3 d_e^2}{150(1-\varepsilon_C)^2} \tag{11}$$

where d_e is the diameter of rock particles in the solid phase, ε_C is the porosity after coking, the expression is given:

$$\varepsilon_C = \varepsilon(1 - c_{Coke}) \tag{12}$$

where ε is the initial porosity.

The effect of coking on diffusion is described as follows based on the definition of diffusion coefficient:

$$D_{Coke} = \varepsilon_C/\varepsilon D_0 \tag{13}$$

2.3. The numerical method and computational conditions

The solution to the above model is incorporated with the Comsol Multiphysics 3.5 software. The proven finite element method (FEM) is used to solve the model. The modeling domain is meshed by the software to be made up of 1302 triangles. The computational conditions and additional parameters are provided in Table 2. As some parameters are sensitive to temperature, their values listed in Table 2 are determined at 473 K. There are three types of boundaries in the modeling domain: the injection well (Γ_{IW}), the producing well (Γ_{EW}), and the outside boundary (Γ_D). The boundary conditions are given separately:

The injection well (Γ_{IW}): stable concentration of oxygen and temperature, pressure equals the injection pressure, that is $P = P_{IW}$, $c = c_0$, $T = T_0$.

The producing well (Γ_{EW}): convective boundary conditions for conservation of mass and energy, pressure equals the extraction pressure, that is $P = P_{EW}$, $\mathbf{n} \cdot (-D\nabla c) = 0$, $\mathbf{n} \cdot (-\lambda \nabla T) = 0$.

The outside boundary (Γ_D): insulation boundary conditions for conservation of mass and energy, pressure equals the initial pressure, that is $P = P_0$, $\mathbf{n} \cdot (-D\nabla c + c\mathbf{u}) = 0$, $-\mathbf{n} \cdot (-\lambda \nabla T) = 0$.

3. Results and discussion

A direct difference between the HTO and LTO of heavy oil is the ignition temperature. The ignition temperature should be higher than the burning point for HTO, as the reservoir has to be firstly ignited; even sometimes, the artificial fire up is required. While for LTO, lower ignition temperature is employed to avoid the coking formation. Herein, the ignition temperatures of high and low temperature oxidation are determined as 673.15 and 473.15 K, respectively.

3.1. Temperature distribution in the HTO process

The temperature distribution of the modeling domain after different durations of oxidation reaction is shown as Fig. 3a–e.

Table 2
The computation conditions and additional parameters.

Parameter	Value	Parameter	Value
P_{IW} (Pa)	10000	ρ_s (kg m^{-3})	2000
P_{EW} (Pa)	−110	λ (W m^{-1} K^{-1})	1.2
D_0 (m^2 s^{-1})	2.014×10^{-6}	c_g (J kg^{-1} K^{-1})	955.19
ε	0.33	κ (m^2)	6.042×10^{-11}
c_s (J kg^{-1} K^{-1})	1095.52	η (Pa s)	3×10^{-5}

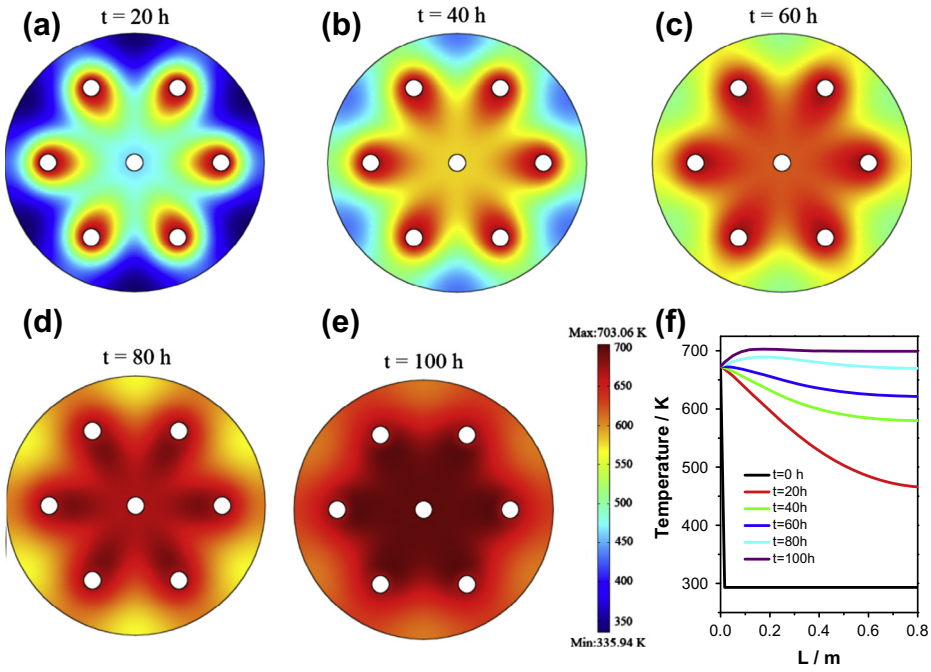

Fig. 3. High temperature oxidation process: The temperature distribution after oxidation reaction for (a) 20 h, (b) 40 h, (c) 60 h, (d) 80 h, (e) 100 h; and (f) the temperature of the region between the injection well and the producing well with reaction time.

An oxidation with a duration of 100 h is simulated. The temperature range in the legend bar for each figure is of the same. The bluish[1] colors represent low temperature with the lowest value of 335.94 K, while the warm colors indicate higher temperature with the highest value of 703.06 K. The modeling domain is gradually heated up with a continuous oxidation (Fig. 3) with the highest reaction temperature at 703.06 K, which is about 30 K higher than the ignition temperature. In contrast, the region between the injection wells and the outside boundary is rather cold, as the low pressure gradient leads to low velocity of oxygen flow according to the Darcy's Law and the low thermal conduction ability of the rocks. Concerning on the region between the injection and the producing well, the rising of temperature with the reaction time is illustrated as Fig. 3f. The initial temperature of the modeling domain is set at 293 K. The *X*-axis means the distance between the injection and producing wells, the injection well is set as the zero point. From the simulation result, the modeling domain is gradually heated up. The temperature rises higher than the ignition temperature after 60 h reaction.

3.2. The temperature distribution for LTO

The temperature distribution of the modeling domain after oxidation reaction for 20, 40, 60, 80, and 100 h in the LTO process is shown as Fig. 4a–e, respectively. The temperature range in the legend bar is ranging from 312.80 to 473.15 K. The temperature of regions around the injection wells rises firstly, then the surrounding regions are heated gradually. The temperature of the regions near the outside boundary is lower than that of the central part, which is attributed from the low oxygen concentration at the boundary. The region between the injection well and the producing well was effectively heated. The temperature of the modeling domain is lower than the injection temperature due to the low reaction rate and few heat. The temperature change of the region between the injection well and the producing well with reaction time is shown in Fig. 4f. The initial temperature is also 293 K. The region is gradually heated with the final temperature of the producing well after 100 h close to the injection temperature.

3.3. HTO vs. LTO: The temperature profiles

The modeling domain can be heated both in the HTO and the LTO, which was unambiguously confirmed by the simulation results of the temperature distribution in the modeling domain (Figs. 3 and 4). However, there are still some differences in their temperature distribution: the temperature in the modeling domain is higher than the injection temperature with long duration in HTO. While in LTO, the temperature in the modeling domain is always lower than the injection temperature. The reason mainly lies in the variety of kinetic of the oxidation reactions and the coking formation reactions. The changes in the oxidation reaction rate constant (k), the molar reaction heat (ΔH) and the coking reaction rate constant (k_c) with temperature are shown in Fig. 5a–c.

As shown in Fig. 5a, the oxidation rate constant increases rapidly with reaction temperature. As k represents reaction rate constant of the reactant, its value is negative. The value of k is quite smaller in the LTO than the HTO. As the heat is generated by the exothermic oxidation reactions, the lower reaction rate leads to smaller amount of released heat, consequently, there is inhomogeneous temperature distribution of the modeling domain. A negative temperature gradient region, from 300 to 350 °C, over which the oxygen reaction rate decreases as the temperature increase is observed. Such phenomenon has been investigated on LTO process by Moore [40]. The reaction oxidation mechanisms in the LTO range is quite different from these in the HTO region.

The molar reaction heat grows with temperature following an exponential function (Fig. 5b). When the ignition temperature rises, the heat produced in the exothermic oxidation reaction dramatically increases. Such energy will heat the oil reservoir, and lead to an increased trend of the temperature distribution.

[1] For interpretation of color in Fig. 3, the reader is referred to the web version of this article.

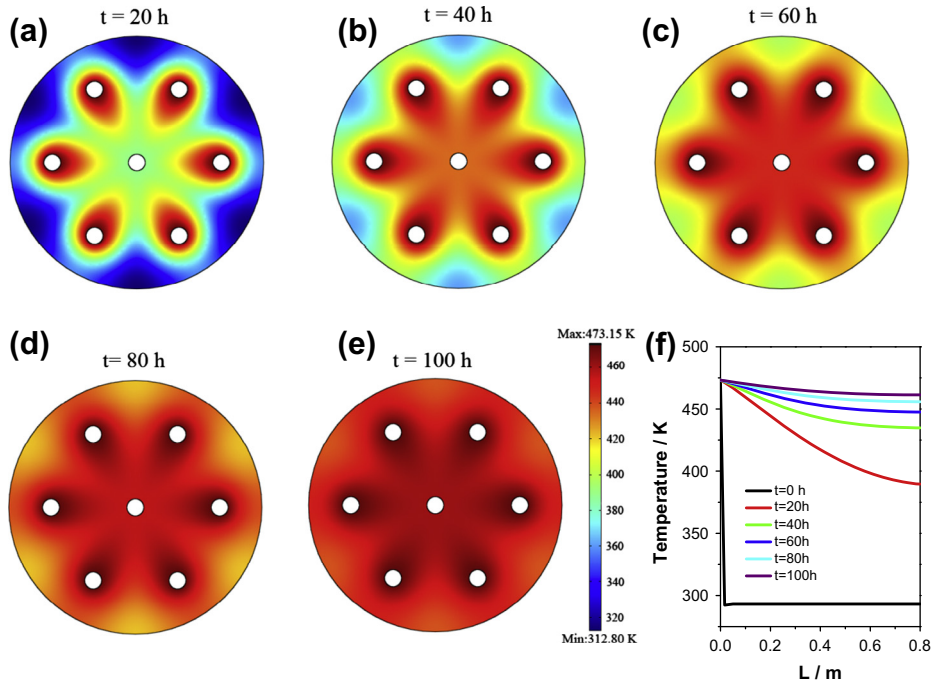

Fig. 4. Low temperature oxidation process: The temperature distribution after oxidation reaction for (a) 20 h, (b) 40 h, (c) 60 h, (d) 80 h, (e) 100 h; and (f) the temperature of the region between the injection well and the producing well with reaction time.

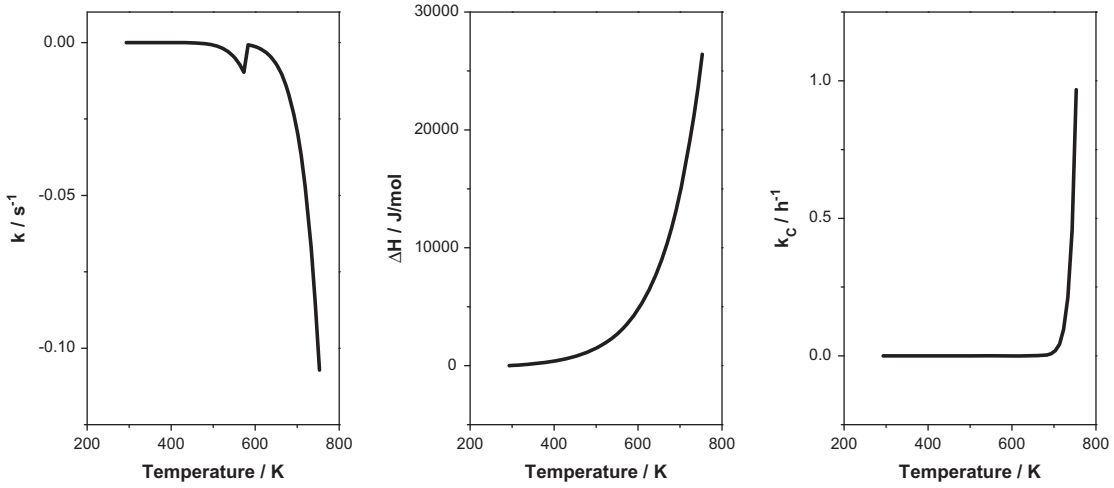

Fig. 5. The profiles of the oxidation reaction rate (k), the molar reaction heat (ΔH) and the coking reaction rate (k_c) with reaction temperature.

The proportion of coke produced is about zero when the temperature is lower than 420 °C, then the coking rate increases drastically (Fig. 5c). There is almost no coking formation as the temperature is lower than the injection temperature (200 °C) during LTO. As a result, the permeability and diffusion coefficient of oxygen were preserved at a high level. This is benefited for the efficient heating of the whole modeling domain. In contrast, the high temperature leads to serious coking in the HTO process. The induced cokes block the flow and diffusion of oxygen. Coking is one of the main problems that affect the efficiency in the flame spread of HTO.

3.4. The governing dimensionless number for the oxidation reaction EOR

The parameters that influence the temperature distribution in the modeling domain during the oil oxidation process are deduced from the above model. The parameters includes: the ignition temperature T_s, the concentration of oxygen in the injection gas c_s, the pressure drop between the injection well and the producing well ΔP, the distance from the injection well to the producing well L, the conduction coefficient λ, the permeability of gas κ, the viscosity of the gas η, the parameters in the kinetic sub-model k and ΔH. Herein two dimensionless numbers integrated based on the above parameters are proposed to describe the governing factors of the oxidation reaction enhanced oil recovery. One of the dimension numbers is the KP number which is defined as follow:

$$\phi = L\sqrt{\frac{k}{\kappa/\eta\Delta p}} \tag{14}$$

The KP number describes the ratio of oxygen consumed in the oxidation reaction to that transported through convection. The distance of the injection well and producing well (L) influences the KP

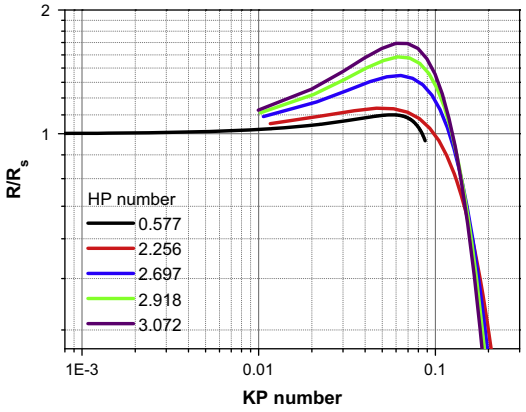

Fig. 6. Correlation of the strength of the oxidation reaction with the KP and HP number.

number. From Figs. 3 and 4b, the temperature of the modeling domain is heated up gradually, the change of temperature is depended on the positions of the modeling domain.

The other dimensionless number named HP number is defined as follow:

$$\beta = \frac{\kappa/\eta \Delta p(-\Delta H)c_S}{\lambda T_S} \tag{15}$$

The HP number mainly describes the effect of heat generated through the oxidation reaction. For exothermic reaction, a negative value of ΔH affords a positive HP number. The value of HP number increases with the reaction heat. Besides, the conduction coefficient λ, the ignition temperature T_s and the oxygen concentration in the injection gas c_s are also integrated.

Correlation of the simulation results using the two dimensionless numbers is shown in Fig. 6. The *X*-axis is the KP number, the *Y*-axis is the ratio of reaction rate at different positions to that at the position next to the injection well, R/R_s, which is influenced by the temperature and the concentration of oxygen. A family profiles that are corresponded to different HP numbers are shown in Fig. 6. The profile with a HP number of 0.577 describes the conditions of LTO. The reaction rate at the whole model domain is approximately similar to that next to the injection well, showing that the oxidation reaction is very smooth for low temperature oxidation. The curves at HP number of 2.256, 2.697, 2.918, and 3.072 are corresponded to the HTO process. The reaction rate is much higher at larger KP number and HP number (Fig. 6).

Fig. 6 can be used as a criterion to describe the oxidation reaction enhanced oil recovery process. At certain operation parameters, the strength of the oxidation reaction at different positions of the reservoir can be judged based on Fig. 6 when the KP number and HP number was determined by the given injection temperature, oxygen concentration, the reservoir condition (*e.g.* the permeability and the conduction coefficient). The proper operation region can also be determined with Fig. 6 when the requirement of the oxidation strength is provided.

4. Conclusions

A mathematic model to describe the *in situ* oxidation of heavy oil in the reservoir is proposed. The process including the flow of gas controlled by the Darcy's law, the conservation of mass and energy together with the kinetic and coking sub-models are considered. The kinetic sub-model is fitted based on the characterization results of the heavy oil using TGA-DSC profile. The coking sub-model as well as the Ergun law is employed to describe the effect of coking on the permeability of gas. Both the HTO and LTO of the heavy oil are effective to heat up the modeling domain. Comparing the temperature distribution of the modeling domain, the LTO offers a uniform temperature throughout the whole reservoir, while the HTO has a high temperature frontier. This is mainly attributed from the significant change in the kinetic and coking formation at low and high reaction temperature. The main parameters that influence the temperature distribution in the oxidation process are integrated to two dimensionless numbers (KP and HP number). The correlation of these two numbers with the strength of oxidation reaction can be employed as guidance for selecting the proper operation region in the oxidation reaction enhanced oil recovery process.

Acknowledgements

The authors thank Prof. Lin Shi at Department of Thermal Engineering, and Prof. Yingying Zhang at Center for Nano and Micro Mechanics, Tsinghua University for helpful discussion. The work was supported by the PetroChina Technology R&D Project on New Technology and Method for Oil & Gas Development (2011A-1006).

References

[1] H.H. Xu, N.E. Okazawa, R.G. Moore, S.A. Mehta, C.J. Laureshen, M.G. Ursenbach, D.G. Mallory, *In situ* upgrading of heavy oil, J. Can. Petrol. Technol. 40 (2001) 45–53.
[2] L.M. Castanier, W.E. Brigham, Upgrading of crude oil *via in situ* combustion, J. Petrol. Sci. Eng. 39 (2003) 125–136.
[3] I.D. Gates, J. Adams, S. Larter, The impact of oil viscosity heterogeneity on the production characteristics of tar sand and heavy oil reservoirs. Part II: Intelligent, geotailored recovery processes in compositionally graded reservoirs, J. Can. Petrol. Technol. 47 (2008) 40–49.
[4] S. Larter, J. Adams, I.D. Gates, B. Bennett, H. Huang, The origin, prediction and impact of oil viscosity heterogeneity on the production characteristics of tar sand and heavy oil reservoirs, J. Can. Petrol. Technol. 47 (2008) 52–61.
[5] Y.L. Chen, Y.Q. Wang, J.Y. Lu, C.A. Wu, The viscosity reduction of nano-keggin-$K_3PMo_{12}O_{40}$ in catalytic aquathermolysis of heavy oil, Fuel 88 (2009) 1426–1434.
[6] M.Z. Dong, S.Z. Ma, Q. Liu, Enhanced heavy oil recovery through interfacial instability: a study of chemical flooding for Brintnell heavy oil, Fuel 88 (2009) 1049–1056.
[7] T.X. Xia, M. Greaves, A.T. Turta, C. Ayasse, THAI – A 'short-distance displacement' *in situ* combustion process for the recovery upgrading of heavy oil, Chem. Eng. Res. Des. 81 (2003) 295–304.
[8] M.V. Kok, R. Ocalan, Modeling of *in-situ* combustion for Turkish heavy crude-oil fields, Fuel 74 (1995) 1057–1060.
[9] R. Ocalan, M.V. Kok, *In situ* combustion model development and its applications for laboratory studies, Fuel 74 (1995) 1632–1635.
[10] N. Mahinpey, A. Ambalae, K. Asghari, *In situ* combustion in enhanced oil recovery (EOR): a review, Chem. Eng. Commun. 194 (2007) 995–1021.
[11] Z.S. Liu, K. Jessen, T.T. Tsotsis, Optimization of *in-situ* combustion processes: a parameter space study towards reducing the CO_2 emissions, Chem. Eng. Sci. 66 (2011) 2723–2733.
[12] M. Dabbous, P.F. Fulton, Low-temperature-oxidation reaction kinetics and effects on the in situ combustion process, SPEJ 14 (1974) 253–262.
[13] Y.H. Shokrlu, Y. Maham, X. Tan, T. Babadagli, M. Gray, Enhancement of the efficiency of *in situ* combustion technique for heavy-oil recovery by application of nickel ions, Fuel 105 (2013) 397–407.
[14] Z. Khansari, I.D. Gates, N. Mahinpey, Low-temperature oxidation of Lloydminster heavy oil: kinetic study and product sequence estimation, Fuel 115 (2014) 534–538.
[15] Z. Khansari, I.D. Gates, N. Mahinpey, Detailed study of low-temperature oxidation of an Alaska heavy oil, Energy Fuels 26 (2012) 1592–1597.
[16] P. Murugan, N. Mahinpey, T. Mani, K. Asghari, Effect of low-temperature oxidation on the pyrolysis and combustion of whole oil, Energy 35 (2010) 2317–2322.
[17] Z. Khansari, P. Kapadia, N. Mahinpey, I.D. Gates, A new reaction model for low temperature oxidation of heavy oil: experiments and numerical modeling, Energy 64 (2014) 419–428.
[18] A. Shah, R. Fishwick, J. Wood, G. Leeke, S. Rigby, M. Greaves, A review of novel techniques for heavy oil and bitumen extraction and upgrading, Energy Environ. Sci. 3 (2010) 700–714.
[19] R. Hashemi, N.N. Nassar, P.P. Almao, Enhanced heavy oil recovery by *in situ* prepared ultradispersed multimetallic nanoparticles: a study of hot fluid flooding for Athabasca Bitumen recovery, Energy Fuels 27 (2013) 2194–2201.

[20] D. Gutierrez, R.G. Moore, M.G. Ursenbach, S.A. Mehta, The ABCs of *in-situ*-combustion simulations: from laboratory experiments to field scale, J. Can. Petrol. Technol. 51 (2012) 256–267.
[21] B. Sequera, R.G. Moore, S.A. Mehta, M.G. Ursenbach, Numerical simulation of *in-situ* combustion experiments operated under low temperature conditions, J. Can. Petrol. Technol. 49 (2010) 55–64.
[22] H. Fadaei, L. Castanier, A.M. Kamp, G. Debenest, M. Quintard, G. Renard, Experimental and numerical analysis of *in-situ* combustion in a fractured core, SPE J. 16 (2011) 358–373.
[23] B.Y. Jamaloei, M.Z. Dong, N. Mahinpey, B.B. Maini, Enhanced cyclic solvent process (ECSP) for heavy oil and Bitumen recovery in thin reservoirs, Energy Fuels 26 (2012) 2865–2874.
[24] C.F. Xi, W.L. Guan, Y.W. Jiang, J.Z. Liang, Y. Zhou, J. Wu, X.C. Wang, H.J. Cheng, J.H. Huang, B.S. Wang, Numerical simulation of fire flooding for heavy oil reservoirs after steam injection: a case study on Block H1 of Xinjiang Oilfield, NW China, Petrol. Explor. Dev. 40 (2013) 766–773.
[25] K.T. Wang, N. Wang, A protein inspired RNA genetic algorithm for parameter estimation in hydrocracking of heavy oil, Chem. Eng. J. 167 (2011) 228–239.
[26] J. Li, G.H. Luo, Y. Chu, F. Wei, Experimental and modeling analysis of NO reduction by CO for a FCC regeneration process, Chem. Eng. J. 184 (2012) 168–175.
[27] Y. Chu, B.Z. Chu, X.B. Wei, Q. Zhang, F. Wei, An emulsion phase condensation model to describe the defluidization behavior for reactions involving gas-volume reduction, Chem. Eng. J. 198 (2012) 364–370.
[28] A.-M. Al-Bahlani, T. Babadagli, Visual analysis of diffusion process during oil recovery using a Hele-Shaw model with hydrocarbon solvents and thermal methods, Chem. Eng. J. 181 (2012) 557–569.
[29] A.-C. Chen, S.-L. Chen, D.-R. Hua, Z. Zhou, Z.-G. Wang, J. Wu, J.-H. Zhang, Diffusion of heavy oil in well-defined and uniform pore-structure catalyst under hydrodemetallization reaction conditions, Chem. Eng. J. 231 (2013) 420–426.
[30] M. Kashir, K. Zhang, G. Achari, R.G. Moore, S.A. Mehta, M.G. Ursenbach, A numerical model simulating the remediation of hydrocarbon-impacted soils using low-temperature oxidation, Environ. Model. Assess. 13 (2008) 265–274.
[31] M.G. Ursenbach, R.G. Moore, S.A. Mehta, Air injection in heavy oil reservoirs – a process whose time has come (again), J. Can. Petrol. Technol. 49 (2010) 48–54.
[32] P. Murugan, N. Mahinpey, T. Mani, N. Freitag, Pyrolysis and combustion kinetics of Fosterton oil using thermogravimetric analysis, Fuel 88 (2009) 1708–1713.
[33] N.N. Nassar, A. Hassan, G. Luna, P. Pereira-Almao, Kinetics of the catalytic thermo-oxidation of asphaltenes at isothermal conditions on different metal oxide nanoparticle surfaces, Catal. Today 207 (2013) 127–132.
[34] C. Fan, C. Zan, Q. Zhang, D.S. Ma, Y. Chu, H. Jiang, L. Shi, F. Wei, The oxidation of heavy oil: thermogravimetric analysis and non-isothermal kinetics using the distributed activation energy model, Fuel Process. Technol. 119 (2014) 146–150.
[35] C. Plato, A.R. Glasgow, Differential scanning calorimetry as a general method for determining purity and heat of fusion of high-purity organics chemicals: application to 95 compounds, Anal. Chem. 41 (1969) 330–336.
[36] A.J. Guo, X.J. Zhang, Z.X. Wang, Simulated delayed coking characteristics of petroleum residues and fractions by thermogravimetry, Fuel Process. Technol. 89 (2008) 643–650.
[37] W. Jiang, G. Cheng, Y. Zhao, L. Cui, C. Li, Processing Sudan thick oil with delayed coking, Petrol. Refinery Eng. 35 (2005) 6–8.
[38] L. Mao, S. Tong, Study on the thermogravimetric analysis and pyrolysis kinetics of coke from delayed coking, Petrol. Process. Petrochem. 42 (2011) 46–49.
[39] S. Ergun, A.A. Orning, Fluid flow through randomly packed columns and fluidized beds, Ind. Eng. Chem. 41 (1949) 1179–1184.
[40] R.G. Moore, New strategies for *in-situ* combustion, J. Can. Petrol. Technol. 32 (1993) 11–13.